NASA TECHNICAL NOTE

NASA TN D-3077

SUPERSONIC FLUTTER OF A THERMALLY STRESSED FLAT PANEL WITH UNIFORM EDGE LOADS

by Harry G. Schaeffer and Walter L. Heard, Jr.

Langley Research Center

Langley Station, Hampton, Va.

NATIONAL AERONAUTICS AND SPACE ADMINISTRATION • WASHINGTON, D. C. • OCTOBER 1965

NASA TN D-3077

SUPERSONIC FLUTTER OF A THERMALLY STRESSED FLAT PANEL WITH UNIFORM EDGE LOADS

By Harry G. Schaeffer and Walter L. Heard, Jr.

Langley Research Center
Langley Station, Hampton, Va.

NATIONAL AERONAUTICS AND SPACE ADMINISTRATION

For sale by the Clearinghouse for Federal Scientific and Technical Information
Springfield, Virginia 22151 – Price $1.00

SUPERSONIC FLUTTER OF A THERMALLY STRESSED FLAT PANEL WITH UNIFORM EDGE LOADS*

By Harry G. Schaeffer and Walter L. Heard, Jr.
Langley Research Center

SUMMARY

35958

The effect of a nonuniform, self-equilibrating stress state associated with a parabolic temperature distribution is included in the flutter analysis of a rectangular, simply supported panel subjected to airflow over one surface and uniform edge loads. Linearized, static, two-dimensional aerodynamics is used in conjunction with thin-plate theory to formulate the problem. Numerical results for a square panel show that nonuniform self-equilibrating stresses are as important as uniform stresses in affecting flutter behavior.

Author

INTRODUCTION

Dynamic instability of thin platelike structures in a gas flow is a problem which has received considerable attention in recent years. As a result of the high velocities attainable by modern aircraft, severe aerodynamic loading of exterior skin panels frequently occurs and can lead to panel flutter. (See, for example, ref. 1.) In the treatment of panel-flutter problems, theoretical investigators have taken into account such effects as panel configuration, flow orientation, boundary conditions, and uniform midplane stress. However, effects of thermally induced, self-equilibrating, midplane stress have not been examined.

It has already been shown in reference 2 that a system of uniform stresses can greatly reduce the flutter speed of an unbuckled panel. The purpose of the present paper is to investigate the effects of a nonuniform, self-equilibrating, stress state on the flutter behavior of a flat, uniformly stressed panel. Since a nonlinear temperature distribution could easily result from aerodynamic effects, it is assumed for the present analysis that the nonuniform stress state is thermally induced by a parabolic temperature distribution which is constant through the thickness. However, the results are valid for any similar system of self-equilibrating midplane stresses.

---

*Part of the information presented herein was offered as a thesis by the second author in partial fulfillment of the requirements for the degree of Master of Science in Engineering Mechanics, Virginia Polytechnic Institute, Blacksburg, Virgina, December 1964.

For the purpose of this analysis the panel is considered to be simply supported against lateral deflections, but unrestrained to inplane displacements at the boundaries. In order to simplify the analysis the aerodynamic forces are assumed to be those resulting from Ackeret theory. The analysis proceeds by using the Galerkin technique in conjunction with an assumed stress function to determine an approximate midplane stress distribution corresponding to the assumed temperature variation and boundary conditions. This thermal stress distribution is then substituted into the linear partial differential equation governing lateral deflections of thin plates in combined bending and compression. The Galerkin procedure is used again to obtain approximate solutions for the flutter behavior, and numerical results are presented for a square panel subjected to various combinations of uniform loading applied at the boundaries.

SYMBOLS

a_{mn} amplitude coefficients (see eq. (11))

a panel length

b panel width

$$C = -\frac{6\left[1 + \left(\frac{a}{b}\right)^2\right]}{1 + \frac{4}{7}\left(\frac{a}{b}\right)^2 + \left(\frac{a}{b}\right)^4}$$

D panel stiffness, $\frac{Eh^3}{12(1 - \mu^2)}$

E Young's modulus

h panel thickness

i,j,m,n,r,s integers

$$k^2 = \frac{\gamma h a^4}{\pi^4 D}\omega^2$$

$(I_1)_{rs},(I_2)_{rs},(I_3)_{rs}$ integrals defined by equations (13b) to (13d)

$$K_{rs} = M_{rs} + P_{rs} - 4Q_{rs} - \frac{1}{40}\left[\left(\frac{r}{s}\right)^2 + \left(\frac{s}{r}\right)^2\right]a_{rs}$$

L_{rs} aerodynamic loading coefficient

l aerodynamic pressure load per unit area

M Mach number

M_{rs} coefficient defined by equation (A5)

N_x, N_y, N_{xy} midplane stress resultants

N_{x_o}, N_{y_o} midplane uniform stress resultants

$N_{x_T}, N_{y_T}, N_{xy_T}$ midplane thermal stress resultants

P_{rs} coefficient defined by equation (A6)

q dynamic pressure

Q_{rs} coefficient defined by equation (A7)

R total number of terms in flow direction

$$R_{x_o} = \frac{N_{x_o} a^2}{\pi^2 D}$$

$$R_{y_o} = \frac{N_{y_o} a^2}{\pi^2 D}$$

S total number of terms in cross-flow direction

t time

T temperature

ΔT_1 maximum amplitude of temperature distribution

w lateral deflection of panel

x,y,z Cartesian coordinates of panel

α coefficient of thermal expansion

γ mass density of panel

$$\delta_{ij} = \begin{cases} 1 & \text{when } i = j \\ 0 & \text{when } i \neq j \end{cases}$$

λ dynamic-pressure parameter, $\dfrac{2qa^3}{D\sqrt{M^2 - 1}}$

λ_{cr} critical value of λ

μ Poisson's ratio

φ Airy stress function

ψ thermal stress parameter, $\dfrac{\alpha E h a^2 \Delta T_1}{\pi^2 D}$

$$\Psi = - \frac{C}{\pi^2}\left(\frac{a}{b}\right)^2 \psi$$

Ω generalized eigenvalue

ω frequency

Notation

$$\nabla^2 = ( )_{,xx} + ( )_{,yy}$$

$$\nabla^4 = ( )_{,xxxx} + 2( )_{,xxyy} + ( )_{,yyyy}$$

When subscripts follow a comma, they indicate partial differentiation of the principal symbol with respect to the subscripts.

STATEMENT OF PROBLEM AND ANALYSIS

A flat, rectangular panel of length a, width b, and uniform thickness h, as shown in figure 1, is considered in this analysis. The panel is simply supported on all edges, exposed to supersonic airflow at Mach number M over one surface, and subjected to a nonlinear temperature distribution $T = T(x,y)$ in the middle plane. The panel edges are considered to be unrestrained to thermal expansion; however, uniform loading, N_{x_o} and N_{y_o}, which is independent of the temperature distribution may be applied at the boundary.

Basic Equations

In this analysis thin-plate theory including the effects of inplane loads is used. The basic equilibrium equations for this case are

$$D\nabla^4 w + N_x w_{,xx} + 2N_{xy} w_{,xy} + N_y w_{,yy} + \gamma h w_{,tt} = 0 \qquad (1)$$

$$\left.\begin{aligned} N_{x,x} + N_{xy,y} &= 0 \\ N_{y,y} + N_{xy,x} &= 0 \end{aligned}\right\} \tag{2}$$

It is assumed that N_x and N_y are positive in compression and that all material properties are to be evaluated at the average panel temperature.

An approximate expression for the aerodynamic pressure load l is obtained by use of linearized, static, two-dimensional aerodynamics (Ackeret theory). This approximation not only greatly simplifies the analysis, but as shown in reference 3, yields essentially the same flutter results as exact aerodynamics at $M \geqq 1.3$ for uniformly stressed panels, except when the stress level causes two modes of oscillation to have the same, or nearly the same, frequency. Thus, if care is taken to avoid these stress levels, Ackeret theory should also be applicable to the nonuniform stress problem of the present analysis, so that

$$l = \frac{-2q}{\sqrt{M^2 - 1}} w,_x \tag{3}$$

The midplane force intensity terms in equations (1) and (2) are written as the sum of those induced by applied, uniform, normal forces at the boundary (subscript o) and those resulting from the nonlinear temperature distribution (subscript T) as follows:

$$\left.\begin{aligned} N_x &= N_{x_o} + N_{x_T} \\ N_y &= N_{y_o} + N_{y_T} \\ N_{xy} &= N_{xy_T} \end{aligned}\right\} \tag{4}$$

The thermally induced stresses are determined in terms of a stress function $\varphi = \varphi(x,y)$ defined by the following relations:

$$\left.\begin{aligned} N_{x_T} &= \varphi,_{yy} \\ N_{y_T} &= \varphi,_{xx} \\ N_{xy_T} &= -\varphi,_{xy} \end{aligned}\right\} \tag{5}$$

This stress function identically satisfies the equilibrium conditions given by equations (2). For compatibility of inplane strains, the stress function must satisfy the following partial differential equation (ref. 4):

$$\nabla^4 \varphi = \alpha E h \nabla^2 T \tag{6}$$

where α is the coefficient of thermal expansion at the average plate temperature and the temperature T is a function of x and y. Note that the sign

of the right-hand side is opposite to that normally encountered, because direct stresses are positive in compression.

The panel boundary conditions have been chosen in such a way that they can be satisfied by using rather simple functions. Thus, the resulting flutter analysis is greatly simplified, but still predicts trends which one may expect to be valid for the actual panel.

The condition that the panel be free from thermally induced normal and shear stresses on the boundaries requires that the stress function satisfy the following boundary conditions:

$$\left.\begin{aligned} &\varphi(0,y) = \varphi(a,y) = \varphi(x,0) = \varphi(x,b) = 0 \\ &\varphi_{,x}(0,y) = \varphi_{,x}(a,y) = \varphi_{,y}(x,0) = \varphi_{,y}(x,b) = 0 \end{aligned}\right\} \tag{7}$$

The condition that the panel boundaries be simply supported requires that the displacement function satisfy the following boundary conditions:

$$\left.\begin{aligned} &w(0,y,t) = w(a,y,t) = w(x,0,t) = w(x,b,t) = 0 \\ &w_{,xx}(0,y,t) = w_{,xx}(a,y,t) = w_{,yy}(x,0,t) = w_{,yy}(x,b,t) = 0 \end{aligned}\right\} \tag{8}$$

The analysis which follows consists of two parts. First, the coefficient of an assumed stress function φ is determined approximately by using the Galerkin technique; then, the stability determinant is determined from the deflection equation, again by using the Galerkin technique.

Solution of Stress Function Equation

The temperature distribution, considered in this problem, varies parabolically in the flow and cross-flow directions and may be represented by

$$T = 16\Delta T_1\left(\frac{x}{a}\right)\left(1 - \frac{x}{a}\right)\left(\frac{y}{b}\right)\left(1 - \frac{y}{b}\right)$$

where ΔT_1 is the maximum amplitude of the temperature distribution.

In order to simplify the subsequent flutter analysis, it is assumed that an approximate stress function is of the following form:

$$\varphi = C\alpha E h a^2 \Delta T_1\left(\frac{x}{a}\right)^2\left(\frac{x}{a} - 1\right)^2\left(\frac{y}{b}\right)^2\left(\frac{y}{b} - 1\right)^2 \tag{9}$$

This approximation of the stress function satisfies all the boundary conditions given by equations (7), but does not satisfy equation (6). The best fit is made by applying the Galerkin technique to equation (6) to evaluate the constant C. The result is

$$C = -\frac{6\left[1 + \left(\frac{a}{b}\right)^2\right]}{1 + \frac{4}{7}\left(\frac{a}{b}\right)^2 + \left(\frac{a}{b}\right)^4} \tag{10}$$

The accuracy of equation (9) in approximating the true stress state associated with the temperature distribution will be assessed subsequently.

Solution of Differential Equation

It is assumed that the solution of equation (1) can be represented as follows:

$$w(x,y,t) = \mathrm{Re} \sum_{m=1}^{\infty} \sum_{n=1}^{\infty} a_{mn} \sin \frac{m\pi x}{a} \sin \frac{n\pi y}{b} e^{i\omega t} \tag{11}$$

where the frequency ω is, in general, complex. Each term of the assumed solution satisfies the given boundary conditions on w.

After substituting equations (3), (4), (5), (10), and (11) into equation (1) and applying the Galerkin procedure, the following set of equations is obtained for the amplitude coefficients a_{mn}:

$$\left\{\left[r^2 + \left(\frac{a}{b}\right)^2 s^2\right]^2 - R_{x_o} r^2 - R_{y_o}\left(\frac{a}{b}\right)^2 s^2 - k^2\right\} a_{rs} + \lambda L_{rs}$$

$$- \frac{4}{\pi^2 D} \frac{a}{b}\left[(I_1)_{rs} + 2\frac{a}{b}(I_2)_{rs} + \left(\frac{a}{b}\right)^2 (I_3)_{rs}\right] = 0 \tag{12}$$

where

$$L_{rs} = \frac{4}{ab\pi^3} \int_0^b \int_0^a \sum_{m=1}^{\infty} \sum_{n=1}^{\infty} m a_{mn} \cos \frac{m\pi x}{a} \sin \frac{r\pi x}{a} \sin \frac{n\pi y}{b} \sin \frac{s\pi y}{b} \, dx \, dy \tag{13a}$$

$$(I_1)_{rs} = \int_0^b \int_0^a \sum_{m=1}^{\infty} \sum_{n=1}^{\infty} m^2 a_{mn} \varphi_{,yy} \sin \frac{m\pi x}{a} \sin \frac{r\pi x}{a} \sin \frac{n\pi y}{b} \sin \frac{s\pi y}{b} \, dx \, dy \tag{13b}$$

$$(I_2)_{rs} = \int_0^b \int_0^a \sum_{m=1}^{\infty} \sum_{n=1}^{\infty} mn a_{mn} \varphi_{,xy} \cos \frac{m\pi x}{a} \sin \frac{r\pi x}{a} \cos \frac{n\pi y}{b} \sin \frac{s\pi y}{b} \, dx \, dy \tag{13c}$$

$$(I_3)_{rs} = \int_0^b \int_0^a \sum_{m=1}^{\infty} \sum_{n=1}^{\infty} n^2 a_{mn} \Phi_{,xx} \sin \frac{m\pi x}{a} \sin \frac{r\pi x}{a} \sin \frac{n\pi y}{b} \sin \frac{s\pi y}{b} \, dx \, dy \quad (13d)$$

$$r = 1, 2, 3, \ldots$$

$$s = 1, 2, 3, \ldots$$

and

$$k^2 = \frac{\gamma h a^4 \omega^2}{\pi^4 D}$$

$$R_{x_o} = \frac{N_{x_o} a^2}{\pi^2 D}$$

$$R_{y_o} = \frac{N_{y_o} a^2}{\pi^2 D}$$

The integrals $(I_1)_{rs}$, $(I_2)_{rs}$, and $(I_3)_{rs}$ which arise due to the nonuniform stress distribution and the integral L_{rs} which arises due to aerodynamic loading are evaluated in appendix A. By using the results of appendix A, equation (12) becomes

$$\left\{\left[r^2 + \left(\frac{a}{b}\right)^2 s^2\right]^2 - R_{x_o} r^2 - R_{y_o}\left(\frac{a}{b}\right)^2 s^2 - k^2 + \frac{C}{5\pi^2}\left(\frac{a}{b}\right)^2\left[\left(\frac{r}{s}\right)^2 + \left(\frac{s}{r}\right)^2\right]\psi\right\} a_{rs}$$

$$+ \lambda L_{rs} + \frac{8C}{\pi^2}\left(\frac{a}{b}\right)^2 \psi K_{rs} = 0 \quad (14)$$

where

$$r = 1, 2, 3, \ldots R$$

$$s = 1, 3, 5, \ldots 2S-1$$

and

$$\psi = \frac{\alpha E h a^2 \Delta T_1}{\pi^2 D}$$

$$K_{rs} = M_{rs} + P_{rs} - 4Q_{rs} - \frac{1}{40}\left[\left(\frac{r}{s}\right)^2 + \left(\frac{s}{r}\right)^2\right]a_{rs}$$

The coefficients L_{rs}, M_{rs}, P_{rs}, and Q_{rs} are defined by equations (A1), (A5), (A6), and (A7), respectively.

The parameter ψ is analogous to the nondimensional, midplane, uniform stress parameters R_{x_o} and R_{y_o} and may be thought of as a thermal stress parameter. The range of the indices r and s is R and 2S-1, respectively, where R is the total number of sine terms in the flow direction and S is the total number of sine terms in the cross-flow direction. Only the sine terms corresponding to an odd number of half waves in the cross-flow direction need to be considered, since, for the symmetric temperature distribution used, even and odd cross-flow terms uncouple and the odd terms lead to the lowest (critical) flutter speed. Thus, equations (14) represent RS (R-times-S) linear, homogeneous, algebraic equations for the RS unknown amplitude coefficients a_{rs}. In order that nontrivial solutions of the system of equations (14) exist, it is necessary that the determinant of coefficients vanish. Thus, the stability criterion may be written in the following form:

$$\det\left(A_{ij} - \Omega\delta_{ij}\right) = 0 \tag{15}$$

where Ω is the eigenvalue.

Since the problem is one of determining the stability of a given form of solution, it is most natural and advantageous to associate the eigenvalue with the frequency parameter k^2. Then, for the nonconservative problem, the system is dynamically unstable when the eigenvalue Ω becomes complex. This implies, according to equation (11), that the system diverges in an oscillating fashion. The problem now is to determine the relationship that must exist between the parameters a/b, R_{x_o}, R_{y_o}, λ, k^2, and ψ in order that the system be stable in the sense described.

For the case where $R = 2$ and $S = 1$, that is,

$$w = \left(a_{11} \sin\frac{\pi x}{a} + a_{21} \sin\frac{2\pi x}{a}\right)\sin\frac{\pi y}{b}\, e^{i\omega t}$$

equation (15) simplifies to the point where it is possible to determine an analytical expression for values of λ corresponding to harmonic motion of the panel. This result is

$$\lambda = \frac{3\pi^4}{8}\left(\left\{R_{x_o} + R_{y_o}\left(\frac{a}{b}\right)^2 + k^2 - \left[1 + \left(\frac{a}{b}\right)^2\right]^2 - \frac{0.4c}{\pi^2}\left(\frac{a}{b}\right)^2\psi\right\}\left\{\left[4 + \left(\frac{a}{b}\right)^2\right]^2 - 4R_{x_o} - R_{y_o}\left(\frac{a}{b}\right)^2 - k^2 + \frac{0.85c}{\pi^2}\left(\frac{a}{b}\right)^2\psi\right\}\right)^{1/2} \tag{16}$$

The critical value of λ can be found by maximizing λ, expression (16), with respect to k^2. Solving for k^2 and substituting the result into equation (16) gives

$$\lambda_{cr} = \frac{9\pi^4}{16}\left|5 - R_{x_o} + 2\left(\frac{a}{b}\right)^2 + \frac{0.15c}{\pi^2}\left(\frac{a}{b}\right)^2\psi\right| \tag{17}$$

where λ_{cr} is the critical value of the dynamic-pressure parameter which leads to flutter.

For higher ordered modal solutions, the algebraic difficulties in obtaining expressions similar to equations (16) and (17) are formidable, and recourse is made to an iterative procedure using a digital computer. For the computer solution the eigenvalues are calculated, and the lowest value of λ for which two of the eigenvalues coalesce is sought. The approximate modal solutions considered are for the cases where $R = 4$, $S = 1$; $R = 6$, $S = 1$; $R = 6$, $S = 2$; and $R = 6$, $S = 3$. The coefficients associated with the latter case have been calculated from equations (14), and the general matrix equation is presented in appendix B. The coefficients associated with the other cases can be determined by deleting appropriate rows and columns.

DISCUSSION OF RESULTS

Thermal Stress Distribution

An approximate stress distribution has been assumed in order to simplify the subsequent dynamic analysis. Since the purpose of this paper is to determine the effect of the stress state associated with a nonlinear temperature distribution on the flutter characteristics, it is important to consider the accuracy with which the stresses obtained from the assumed stress function approximate the true stress state. The true stress state associated with the parabolic temperature distribution has been determined by the finite-difference method of reference 5.

Comparisons between the one-term approximation and a finite-difference solution are presented in figures 2 and 3. Figure 2 shows the variation of N_{x_T} with x for specified values of y, and figure 3 shows the variation of N_{xy_T} with x for specified values of y. The normal stress determined by the

one-term approximation and that determined by the finite-difference solution agree quite well (fig. 2). In the case of the shear stress distribution (fig. 3), the agreement in magnitude is not as close as that for the direct stresses; however, it appears that the agreement is sufficiently close so that the overall results can be interpreted with confidence.

Effect of Temperature Distribution on Flutter Boundary

The effect of the parabolic temperature distribution on the flutter behavior of a square panel free of uniform midplane stress is shown in figure 4. The results are presented for a 6-by-3 ($R = 6$; $S = 3$) term solution. The intersection of the flutter boundary with the λ-axis is the value of λ_{cr} associated with the unstressed, unheated panel. This value decreases as ψ increases (ΔT_1 increases) until the flutter boundary becomes tangent to the curve labeled "thermal buckling loop."

The three regions shown in figure 4 are characterized by the value of the frequency parameter squared (k^2). In the region labeled "panel flat, no flutter," k^2 is real and positive; hence, ω is real. In the region labeled "flutter," k^2 is complex; thus, ω is complex and at least one root will lead to oscillating, divergent panel motion. In the region labeled "panel buckled, no flutter," k^2 is negative; thus, ω is pure imaginary and the panel is statically unstable.

These three regions are separated by two boundaries. The first is the buckling loop which is the locus of points for which $k^2 = 0$. The second is the flutter boundary which is the locus of points at which two frequencies coalesce. The flutter boundary is terminated at its point of tangency with the static buckling loop, since this point represents the limit of linear plate theory. This transition point is of considerable importance, because experience has shown that it represents the lowest value of λ_{cr} associated with this panel configuration.

Figure 4 shows that the stress distribution associated with a parabolic temperature distribution can cause a 61-percent reduction in the value of λ_{cr} associated with an unheated, unstressed panel. In order to give an indication of the magnitude of ΔT_1 which causes an effect of this order, ΔT_1 is computed for a representative square aluminum panel with $\frac{a}{h} = 300$. The results show that a temperature difference of only 27° F between the center and the edges of the panel causes the 61-percent reduction in λ_{cr}.

The effect of the parabolic temperature distribution on the flutter boundary associated with uniform compressive loads in the flow direction is shown in figure 5 for the 6-by-3 term analysis. The curve labeled "$\psi = 0$" is essentially the exact solution established in reference 2 and shows how the critical value of the dynamic-pressure parameter varies with applied uniform loading in the flow direction. Increasing values of ψ lower the flutter boundary.

The regions of stability and instability are not shown in figure 5 but are similar to those shown in figure 4; however, in figure 5 the dynamic-pressure parameter is plotted against R_{x_o} instead of ψ. For every curve represented by some constant value of ψ, there is an associated buckling loop. The dashed line represents the locus of points where the flutter boundary becomes tangent to its corresponding buckling loop.

The decrease in λ_{cr} due to a parabolic temperature distribution is of the same order of magnitude as the decrease in λ_{cr} due to a uniform compressive load in the x-direction. The comparable reductions in λ_{cr} due to the two different parameters indicate that the effect of the nonuniform temperature distribution is as important as that of uniform compressive stress. Since the nonuniform stress distribution could have resulted from causes other than a temperature distribution, the previous statement can be generalized to say that any system of nonuniform self-equilibrating stresses may have a significant effect on panel flutter behavior.

Reference 2 shows that uniform compressive loads applied perpendicular to the direction of airflow have virtually no effect on the flutter of a uniformly stressed panel. It is of interest, therefore, to investigate the effect of R_{y_o} for the present case. In figure 6 the relation between λ_{cr} and R_{x_o} is presented for various values of the stress ratio R_{y_o}/R_{x_o}. The differences in the flutter boundaries due to R_{y_o} are not significant and cannot be plotted on the scale presented. However, the transition point between the flat-panel and the buckled-panel flutter boundaries is significantly affected as indicated by the loci of termination points of the flat-panel flutter boundaries. Thus, for the given range of parameters and the assumed nonuniform stress distribution, the results of figure 5 may be used to predict the flutter behavior of a square panel with good accuracy for any combination of R_{x_o}, R_{y_o}, and ψ which does not cause the panel to buckle. Only the terminal points need to be located. The loci of these terminal points for several values of the stress ratio are shown in figure 6. The curves apply for the stress-ratio range $0 \leqq \frac{R_{y_o}}{R_{x_o}} \leqq 1$ only, since large positive values and large negative values of the ratio may yield different results because of changes in buckling mode shapes in the cross-flow direction. When $\frac{R_{y_o}}{R_{x_o}} = 1$, the locus of termination points of the flat-panel flutter boundary is essentially a horizontal line. Thus for this stress ratio, the theory predicts that the transition point is essentially independent of the relative magnitudes of applied uniform stress and thermal stress.

Since the results presented in this paper were obtained by applying the Galerkin technique, there may be some question as to convergence toward the exact solution of the problem. In order to investigate the question of convergence, results for various approximate solutions are presented in figure 7. The flutter boundaries of λ_{cr} as a function of R_{x_o} for values of

ψ of 10, 20, 30, and 40 are presented in figure 7 for the 2-by-1, 4-by-1, 6-by-1, 6-by-2, and 6-by-3 term analyses. The solid curves represent results of the 6-by-2 and 6-by-3 term analyses whereas the other curves represent the results of the lower order solutions.

An examination of figure 7 shows that the flutter boundary is significantly altered when the number of terms in the flow direction is increased from two to four. However, a further increase to six terms exhibits very little effect; thus, the solution is assumed to be converged for flow-wise terms. The requirement of relatively few flow-wise terms for convergence is not unexpected, since for this range of parameters a four-term solution gave a close approximation to the exact solution in reference 2 where ψ is zero.

Inclusion of two cross-flow terms in the analysis instead of only one exhibits only a very slight lowering of the flutter boundary as may be seen by comparison of the 6-by-1 and 6-by-2 solutions. (For the scale shown, the 6-by-1 and 4-by-1 results are coincident except in fig. 7(a) where the 6-by-1 solution gives the higher values of λ_{cr}.) Inclusion of three cross-flow terms gives essentially the same results as the 6-by-2 solution and indicates that the 6-by-2 solution is converged for the range of ψ considered.

CONCLUDING REMARKS

Nonuniform stresses associated with a parabolic temperature distribution are shown to be as important in affecting panel flutter behavior as uniform loading applied in the direction of airflow. It is also shown that although uniform loading applied perpendicular to the direction of airflow has virtually no effect on the flutter boundaries for values of the stress ratio R_{y_o}/R_{x_o} from 0 to 1, the transition point between the flat-panel flutter boundary and the buckled-panel flutter boundary is significantly affected. As this stress ratio approaches the value of 1, the transition point becomes essentially independent of relative magnitudes of applied uniform loading and thermal stress.

Because of the effects of the nonuniform stresses shown herein, it appears that thermally induced nonuniform stresses should be considered in the correlation of experimental flutter results with theory. In fact, consideration should be given to any system of nonuniform, self-equilibrating stresses, even those resulting from causes other than a nonlinear temperature distribution.

Langley Research Center,
National Aeronautics and Space Administration,
Langley Station, Hampton, Va., August 12, 1965.

APPENDIX A

LOAD COEFFICIENTS

Evaluation of the integral resulting from the aerodynamic loading (eq. (13a)) gives the following expression:

$$L_{rs} = \frac{2}{\pi^4} \sum_{\substack{m=1 \\ m \neq r}}^{R} \frac{rma_{ms}\left[1 - (-1)^{r+m}\right]}{r^2 - m^2} \tag{A1}$$

where the notation $m \neq r$ indicates that the terms in the sum associated with $m = r$ are to be omitted.

The integrals $(I_1)_{rs}$, $(I_2)_{rs}$, and $(I_3)_{rs}$ given by equations (13b), (13c), and (13d), respectively, are evaluated by making use of the specific definition of the stress function given by equation (9). The result is

$$(I_1)_{rs} = -\frac{2C\alpha Eha^3\Delta T_1}{\pi^2 b} M_{rs} \tag{A2}$$

$$(I_2)_{rs} = \frac{4C\alpha Eha^2\Delta T_1}{\pi^2} Q_{rs} \tag{A3}$$

$$(I_3)_{rs} = -\frac{2C\alpha Ehab\Delta T_1}{\pi^2} P_{rs} \tag{A4}$$

where

$$\begin{aligned} M_{rs} = {} & \sum_{\substack{m=1 \\ m \neq r}}^{R} \sum_{\substack{n=1,3 \\ n \neq s}}^{2S-1} a_{mn} \left\{ \frac{72m^2ns\left[(-1)^{n+s} + 1\right]\left[(-1)^{m+r} + 1\right]\left[(m+r)^4 - (m-r)^4\right]}{\pi^4(n-s)^2(n+s)^2(m+r)^4(m-r)^4} \right\} \\ & - \frac{12}{\pi^2}\left[\frac{(r\pi)^2}{60} + \frac{3}{4(r\pi)^2}\right] \sum_{\substack{n=1,3 \\ n \neq s}}^{2S-1} \frac{ns\left[(-1)^{n+s} + 1\right]a_{rn}}{(n-s)^2(n+s)^2} \\ & - \frac{9}{s^2\pi^4} \sum_{\substack{m=1 \\ m \neq r}}^{R} \frac{m^2\left[(-1)^{m+r} + 1\right]\left[(m+r)^4 - (m-r)^4\right]a_{ms}}{(m+r)^4(m-r)^4} \\ & + \frac{3}{2}\left(\frac{r}{s}\right)^2\left[\frac{1}{60} + \frac{3}{4(r\pi)^4}\right]a_{rs} \end{aligned} \tag{A5}$$

APPENDIX A

$$P_{rs} = \sum_{\substack{m=1 \\ m\neq r}}^{R} \sum_{\substack{n=1,3 \\ n\neq s}}^{2S-1} a_{mn} \left\{ \frac{72n^2mr\left[(-1)^{m+r}+1\right]\left[(-1)^{n+s}+1\right]\left[(n+s)^4-(n-s)^4\right]}{\pi^4(n-s)^4(n+s)^4(m+r)^2(m-r)^2} \right\}$$

$$- \frac{12}{\pi^2}\left[\frac{(s\pi)^2}{60} + \frac{3}{4(s\pi)^2}\right] \sum_{\substack{m=1 \\ m\neq r}}^{R} \frac{mr\left[(-1)^{m+r}+1\right]a_{ms}}{(m-r)^2(m+r)^2}$$

$$- \frac{9}{r^2\pi^4} \sum_{\substack{n=1,3 \\ n\neq s}}^{2S-1} \frac{n^2\left[1+(-1)^{n+s}\right]\left[(n+s)^4-(n-s)^4\right]}{(n+s)^4(n-s)^4} a_{rn}$$

$$+ \frac{3}{2}\left(\frac{s}{r}\right)^2\left[\frac{1}{60} + \frac{3}{4(s\pi)^4}\right]a_{rs} \qquad \text{(A6)}$$

$$Q_{rs} = \sum_{\substack{m=1 \\ m\neq r}}^{R} \sum_{\substack{n=1,3 \\ n\neq s}}^{2S-1} \frac{9mn}{\pi^4} a_{mn}\left[(-1)^{n+s}+1\right]\left[(-1)^{m+r}+1\right]$$

$$\times \left\{\left[\frac{(s-n)^3+(s+n)^3}{(s-n)^3(s+n)^3}\right]\left[\frac{(r-m)^3+(r+m)^3}{(r+m)^3(r-m)^3}\right]\right\}$$

$$+ \frac{9}{4\pi^4s^2} \sum_{\substack{m=1 \\ m\neq r}}^{R} m\left[(-1)^{m+r}+1\right]\left[\frac{(r-m)^3+(r+m)^3}{(r-m)^3(r+m)^3}\right]a_{ms}$$

$$+ \frac{9}{4\pi^4r^2} \sum_{\substack{n=1,3 \\ n\neq s}}^{2S-1} n\left[(-1)^{n+s}+1\right]\left[\frac{(s-n)^3+(s+n)^3}{(s-n)^3(s+n)^3}\right]a_{rn}$$

$$+ \frac{9}{16\pi^4r^2s^2} a_{rs} \qquad \text{(A7)}$$

As in equation (A1), the notation $m \neq r$, $n \neq s$ indicates that the terms in the sums associated with $m = r$ and $n = s$ are to be omitted.

APPENDIX B

MATRIX EQUATION FOR THE UNKNOWN AMPLITUDE COEFFICIENTS, a_{mn}

The matrix equation for the case in which six terms in the flow direction and three terms in the cross-flow direction are utilized is as follows:

$$\begin{bmatrix}
Z_{11} & -0.02737\lambda & 0.51380\Psi & -0.01095\lambda & 0.07519\Psi & -0.00704\lambda & 0.51380\Psi & 0 & 0.10394\Psi & 0 & 0.01818\Psi & 0 & 0.07519\Psi & 0 & 0.01818\Psi & 0 & 0.00356\Psi & 0 \\
0.02737\lambda & Z_{21} & -.04927\lambda & 1.00818\Psi & -.01955\lambda & .12845\Psi & 0 & 0.69095\Psi & 0 & 0.08042\Psi & 0 & 0.02599\Psi & 0 & 0.12296\Psi & 0 & 0.00729\Psi & 0 & .00454\Psi \\
.51380\Psi & .04927\lambda & Z_{31} & -.07039\lambda & 1.66544\Psi & -.02737\lambda & -1.19535\Psi & 0 & 1.39042\Psi & 0 & -.06902\Psi & 0 & -.19035\Psi & 0 & .25527\Psi & 0 & -.02815\Psi & 0 \\
.01095\lambda & 1.00818\Psi & .07039\lambda & Z_{41} & -.09124\lambda & 2.50170\Psi & 0 & -1.97278\Psi & 0 & 2.42274\Psi & 0 & -.35191\Psi & 0 & -.32224\Psi & 0 & .44741\Psi & 0 & -.08871\Psi \\
.07519\Psi & .01955\lambda & 1.66544\Psi & .09124\lambda & Z_{51} & -.11198\lambda & -.19035\Psi & 0 & -2.83001\Psi & 0 & 3.76455\Psi & 0 & -.02990\Psi & 0 & -.47128\Psi & 0 & .69634\Psi & 0 \\
.00704\lambda & .12845\Psi & .02737\lambda & 2.50170\Psi & .11198\lambda & Z_{61} & 0 & -.29884\Psi & 0 & -3.81114\Psi & 0 & 5.41011\Psi & 0 & -.04759\Psi & 0 & -.64390\Psi & 0 & 1.00132\Psi \\
.51380\Psi & 0 & -1.19535\Psi & 0 & -.19035\Psi & 0 & Z_{13} & -.02737\lambda & 1.39042\Psi & -.01095\lambda & .25527\Psi & -.00704\lambda & 1.66544\Psi & 0 & -.06902\Psi & 0 & -.02815\Psi & 0 \\
0 & .69095\Psi & 0 & -1.97278\Psi & 0 & -.29884\Psi & .02737\lambda & Z_{23} & -.04927\lambda & 1.69227\Psi & -.01955\lambda & .34761\Psi & 0 & 1.11949\Psi & 0 & .08929\Psi & 0 & -.01726\Psi \\
.10394\Psi & 0 & 1.39042\Psi & 0 & -2.83001\Psi & 0 & 1.39042\Psi & .04927\lambda & Z_{33} & -.07039\lambda & 1.85172\Psi & -.02737\lambda & -2.83001\Psi & 0 & 1.85172\Psi & 0 & .16241\Psi & 0 \\
0 & .08042\Psi & 0 & 2.42274\Psi & 0 & -3.81114\Psi & .01095\lambda & 1.69227\Psi & .07039\lambda & Z_{43} & -.09124\lambda & 1.98463\Psi & 0 & -4.27375\Psi & 0 & 3.09237\Psi & 0 & .09126\Psi \\
.01818\Psi & 0 & -.06902\Psi & 0 & 3.76455\Psi & 0 & .25527\Psi & .01955\lambda & 1.85172\Psi & .09124\lambda & Z_{53} & -.11198\lambda & -.47128\Psi & 0 & -5.70469\Psi & 0 & 4.74662\Psi & 0 \\
0 & .02599\Psi & 0 & -.35191\Psi & 0 & 5.41011\Psi & .00704\lambda & .34761\Psi & .02737\lambda & 1.98463\Psi & .11198\lambda & Z_{63} & 0 & -.70750\Psi & 0 & -7.25959\Psi & 0 & 6.79105\Psi \\
.07519\Psi & 0 & -.19035\Psi & 0 & -.02990\Psi & 0 & 1.66544\Psi & 0 & -2.83001\Psi & 0 & -.47128\Psi & 0 & Z_{15} & -.02737\lambda & 3.76455\Psi & -.01095\lambda & .69634\Psi & -.00704\lambda \\
0 & .12296\Psi & 0 & -.32224\Psi & 0 & -.04759\Psi & 0 & 1.11949\Psi & 0 & -4.27375\Psi & 0 & -.70750\Psi & .02737\lambda & Z_{25} & -.04927\lambda & 4.47766\Psi & -.01955\lambda & .94114\Psi \\
.01818\Psi & 0 & .25527\Psi & 0 & -.47128\Psi & 0 & -.06902\Psi & 0 & 1.85172\Psi & 0 & -5.70469\Psi & 0 & 3.76455\Psi & .04927\lambda & Z_{35} & -.07039\lambda & 4.74662\Psi & -.02737\lambda \\
0 & .00729\Psi & 0 & .44741\Psi & 0 & -.64390\Psi & 0 & .08929\Psi & 0 & 3.09237\Psi & 0 & -7.25959\Psi & .01095\lambda & 4.47766\Psi & .07039\lambda & Z_{45} & -.09124\lambda & 4.89239\Psi \\
.00356\Psi & 0 & -.02815\Psi & 0 & .69634\Psi & 0 & -.02815\Psi & 0 & .16241\Psi & 0 & 4.74662\Psi & 0 & .69634\Psi & .01955\lambda & 4.74662\Psi & .09124\lambda & Z_{55} & -.11198\lambda \\
0 & .00454\Psi & 0 & -.08871\Psi & 0 & 1.00132\Psi & 0 & -.01726\Psi & 0 & .09126\Psi & 0 & 6.79105\Psi & .00704\lambda & .94114\Psi & .02737\lambda & 4.89239\Psi & .11198\lambda & Z_{65}
\end{bmatrix}
\begin{bmatrix} a_{11} \\ a_{21} \\ a_{31} \\ a_{41} \\ a_{51} \\ a_{61} \\ a_{13} \\ a_{23} \\ a_{33} \\ a_{43} \\ a_{53} \\ a_{63} \\ a_{15} \\ a_{25} \\ a_{35} \\ a_{45} \\ a_{55} \\ a_{65} \end{bmatrix} = \{0\} \tag{B1}$$

where the general diagonal elements of the matrix A_{ij} are

$$Z_{rs} = \left[r^2 + \left(\frac{a}{b}\right)^2 s^2\right]^2 - R_{x_o} r^2 - R_{y_o}\left(\frac{a}{b}\right)^2 s^2 - k^2 + \frac{C}{5\pi^2}\left(\frac{a}{b}\right)^2\left[\left(\frac{r}{s}\right)^2 + \left(\frac{s}{r}\right)^2\right]\Psi \tag{B2}$$

and $\Psi = -\frac{C}{\pi^2}\left(\frac{a}{b}\right)^2 \Psi$.

REFERENCES

1. Kordes, Eldon E.; and Noll, Richard B.: Flight Flutter Results for Flat Rectangular Panels. NASA TN D-1058, 1962.

2. Hedgepeth, John M.: Flutter of Rectangular Simply Supported Panels at High Supersonic Speeds. J. Aeron. Sci., vol. 24, no. 8, Aug. 1957, pp. 563-573, 586.

3. Bohon, Herman L.; and Dixon, Sidney C.: Some Recent Developments in Flutter of Flat Panels. J. Aircraft, vol. 1, no. 5, Sept.-Oct. 1964, pp. 280-288.

4. Boley, Bruno A.; and Weiner, Jerome H.: Theory of Thermal Stresses. John Wiley & Sons, Inc., c.1960, pp. 379-382.

5. Schaeffer, Harry G.; and Heard, Walter L., Jr.: Evaluation of an Energy Method Using Finite Differences for Determining Thermal Midplane Stresses in Plates. NASA TN D-2439, 1964.

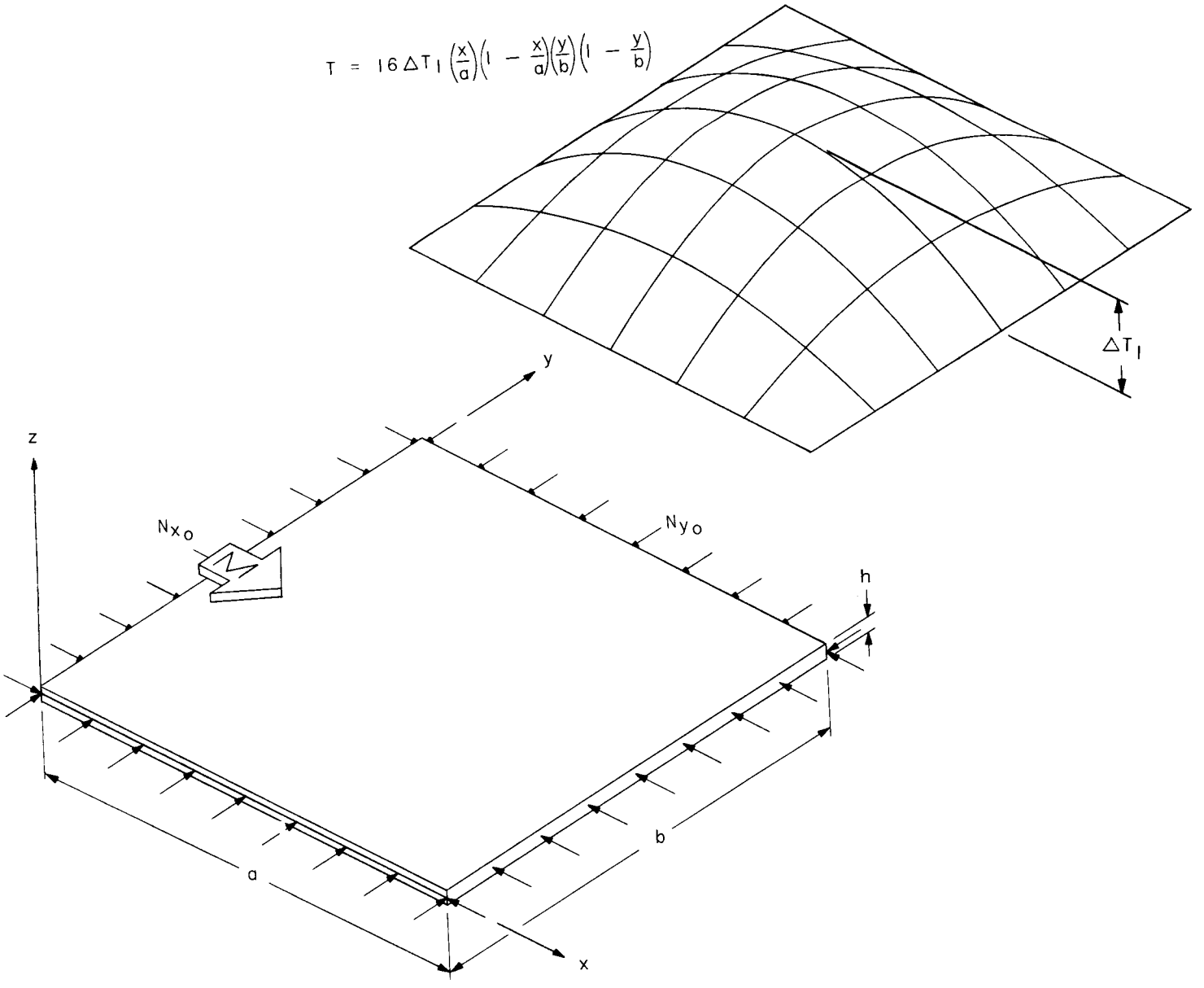

Figure 1.- Panel geometry and temperature distribution.

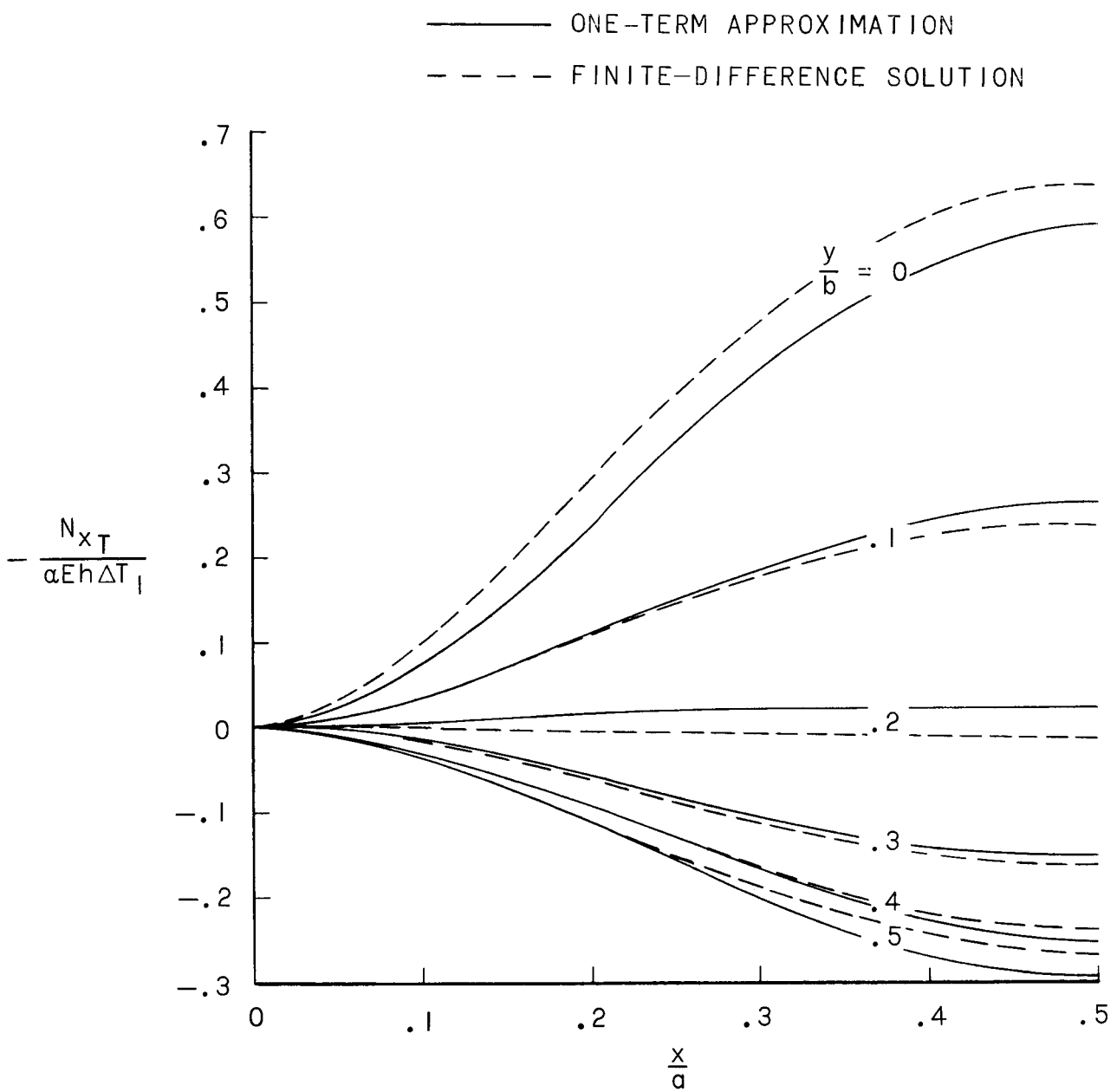

Figure 2.- Variation of stress resultant N_{xT} with x. $T = 16\Delta T_1\left(\frac{x}{a}\right)\left(1 - \frac{x}{a}\right)\left(\frac{y}{b}\right)\left(1 - \frac{y}{b}\right)$; $\frac{a}{b} = 1$; symmetric about $\frac{x}{a} = 0.5$ and $\frac{y}{b} = 0.5$.

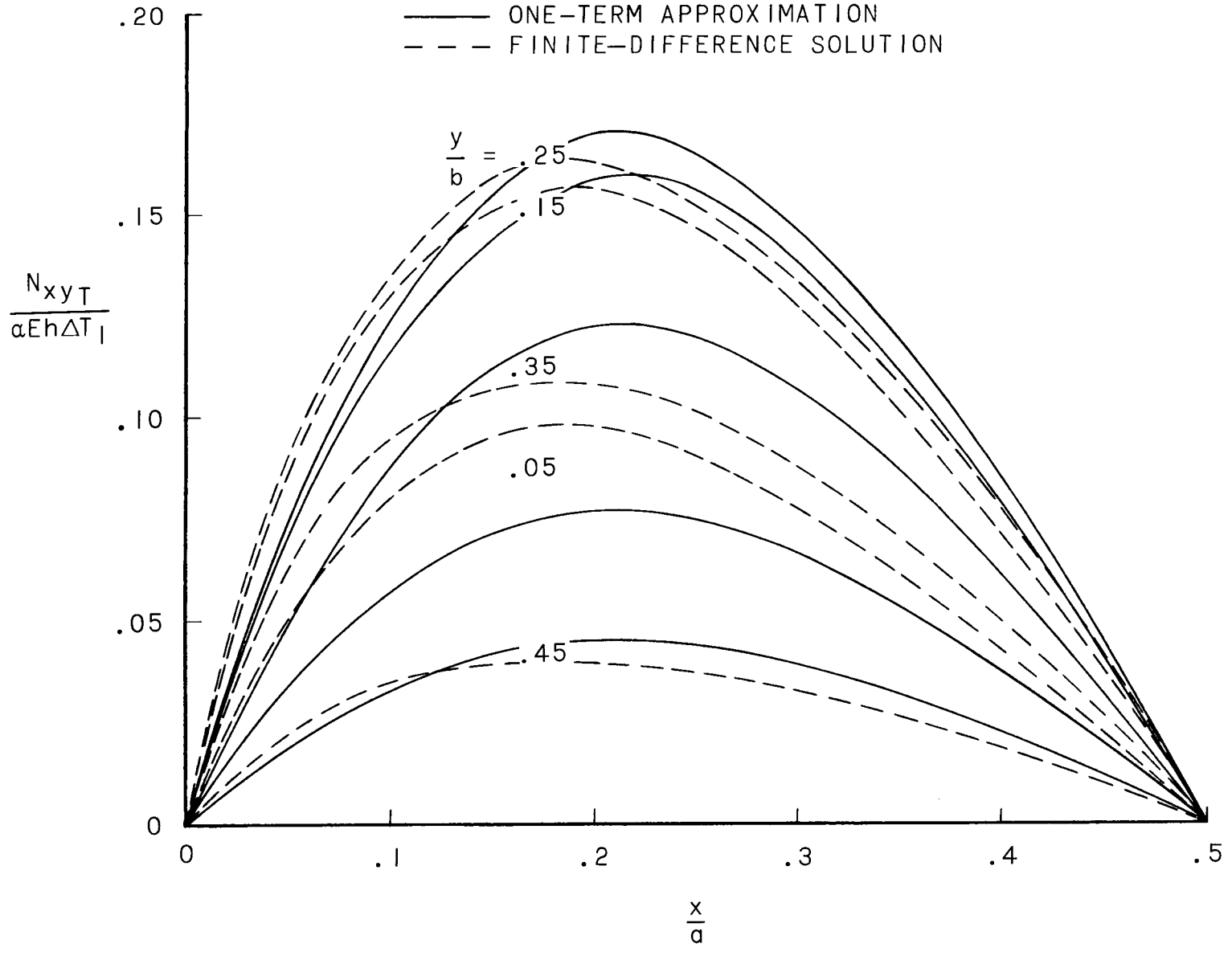

Figure 3.- Variation of shear stress resultant N_{xy_T} with x. $T = 16\Delta T_1\left(\frac{x}{a}\right)\left(1 - \frac{x}{a}\right)\left(\frac{y}{b}\right)\left(1 - \frac{y}{b}\right)$; $\frac{a}{b} = 1$; antisymmetric about $\frac{x}{a} = 0.5$ and $\frac{y}{b} = 0.5$.

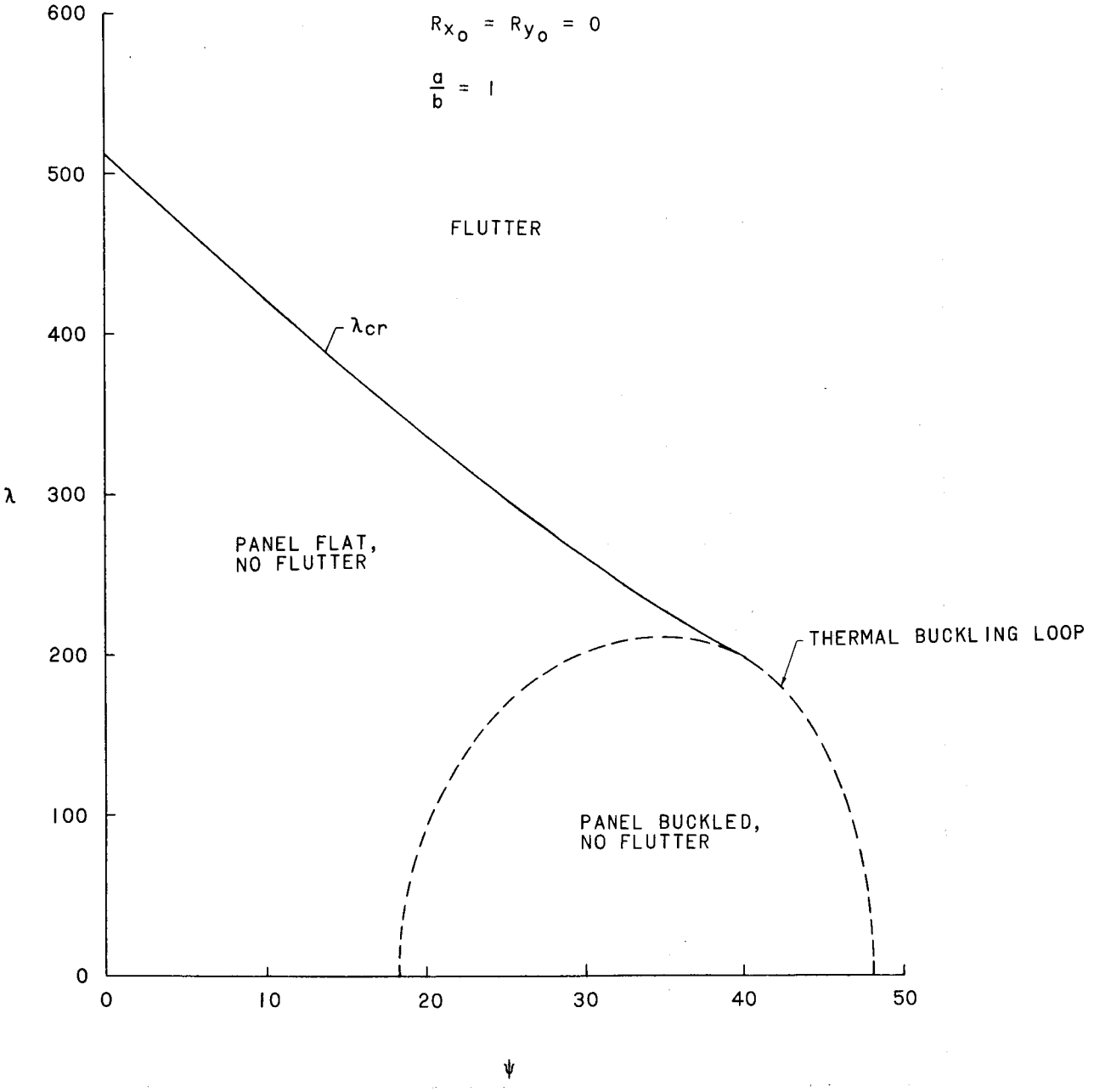

Figure 4.- Thermal flutter boundary for square panel with no externally applied forces.

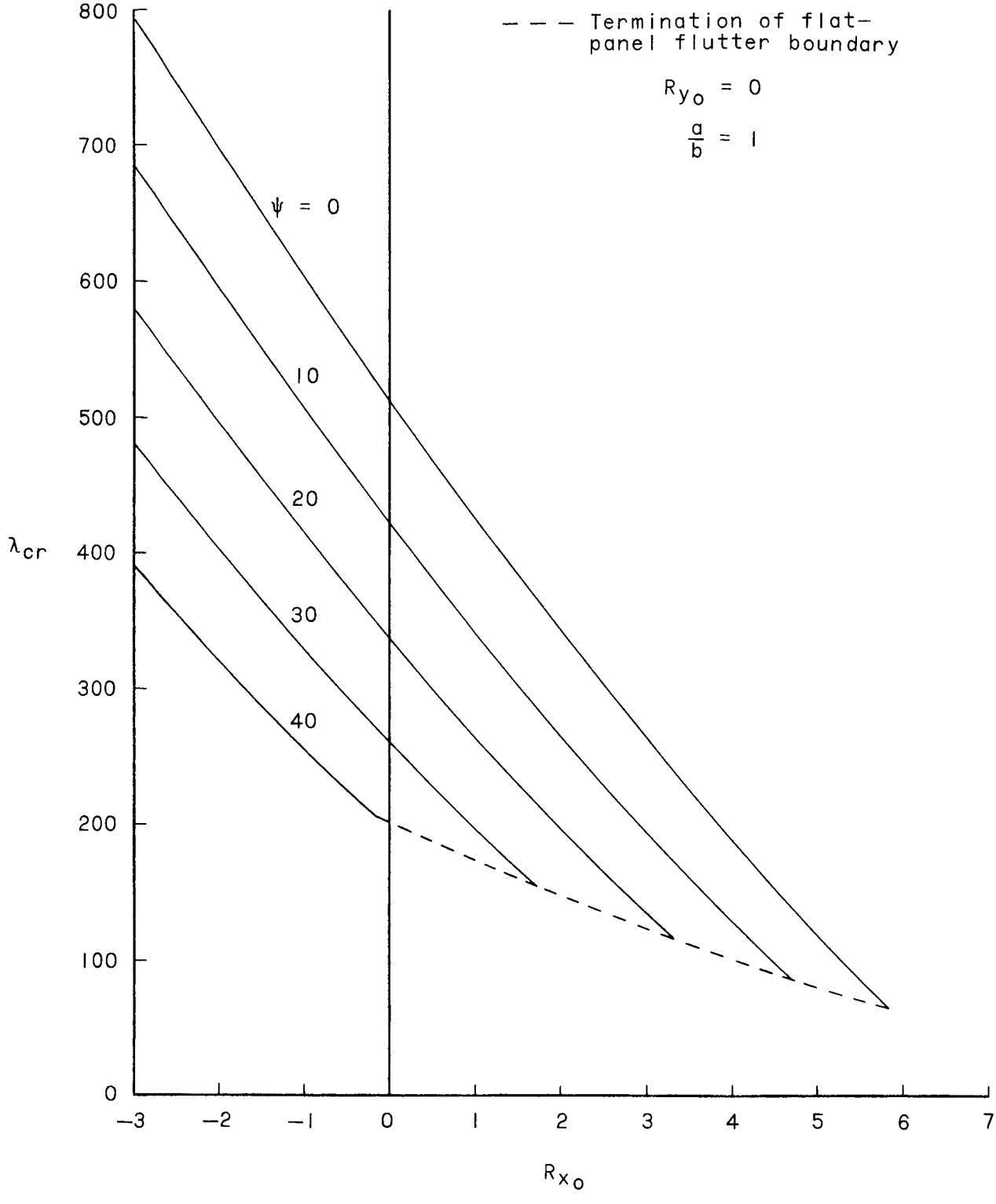

Figure 5.- Effect of thermal stress parameter ψ on flutter boundary of a square panel with uniform edge loads in flow direction.

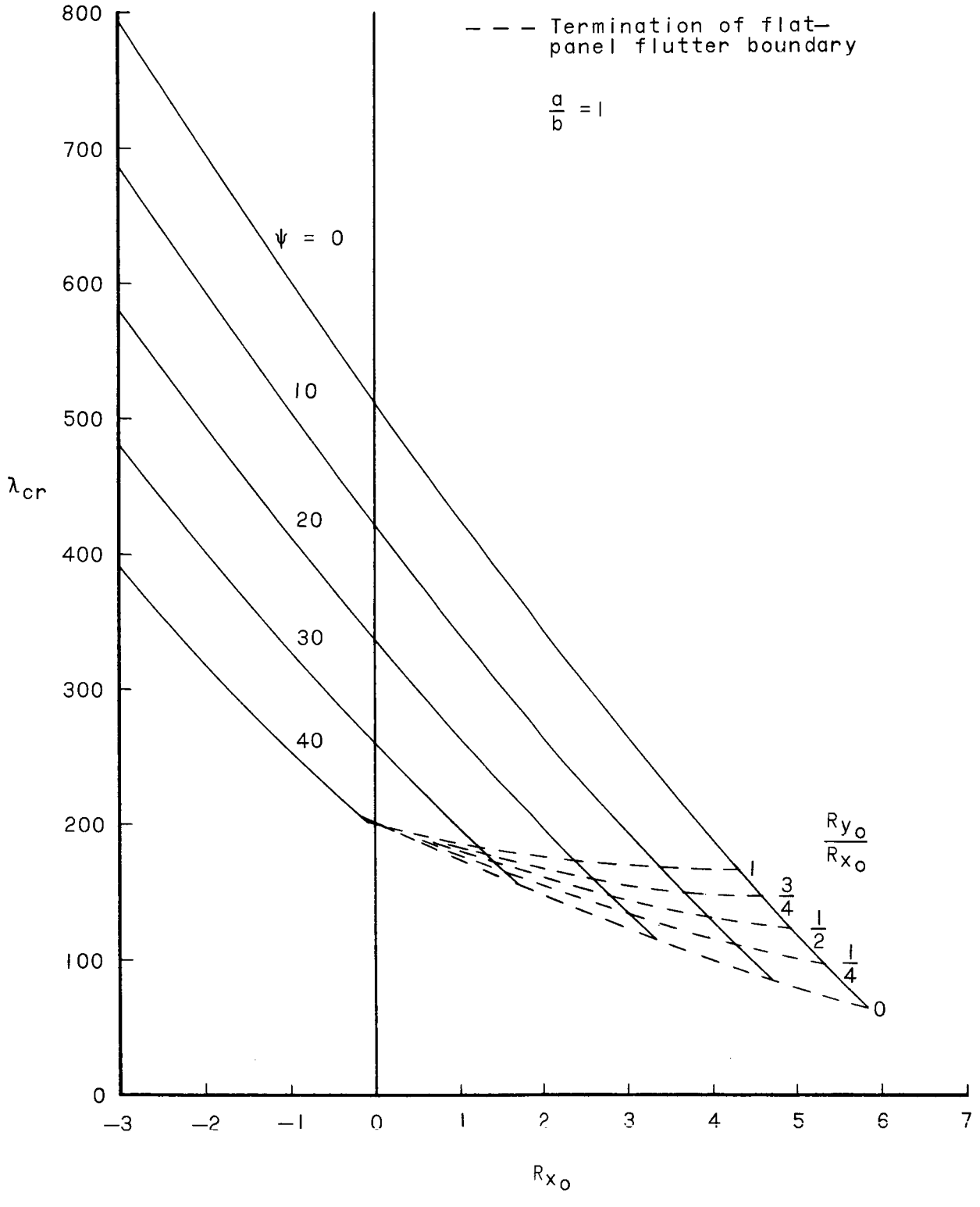

Figure 6.- Effect of thermal stress parameter ψ on flutter boundary of a square panel with uniform edge loads in x- and y-directions.

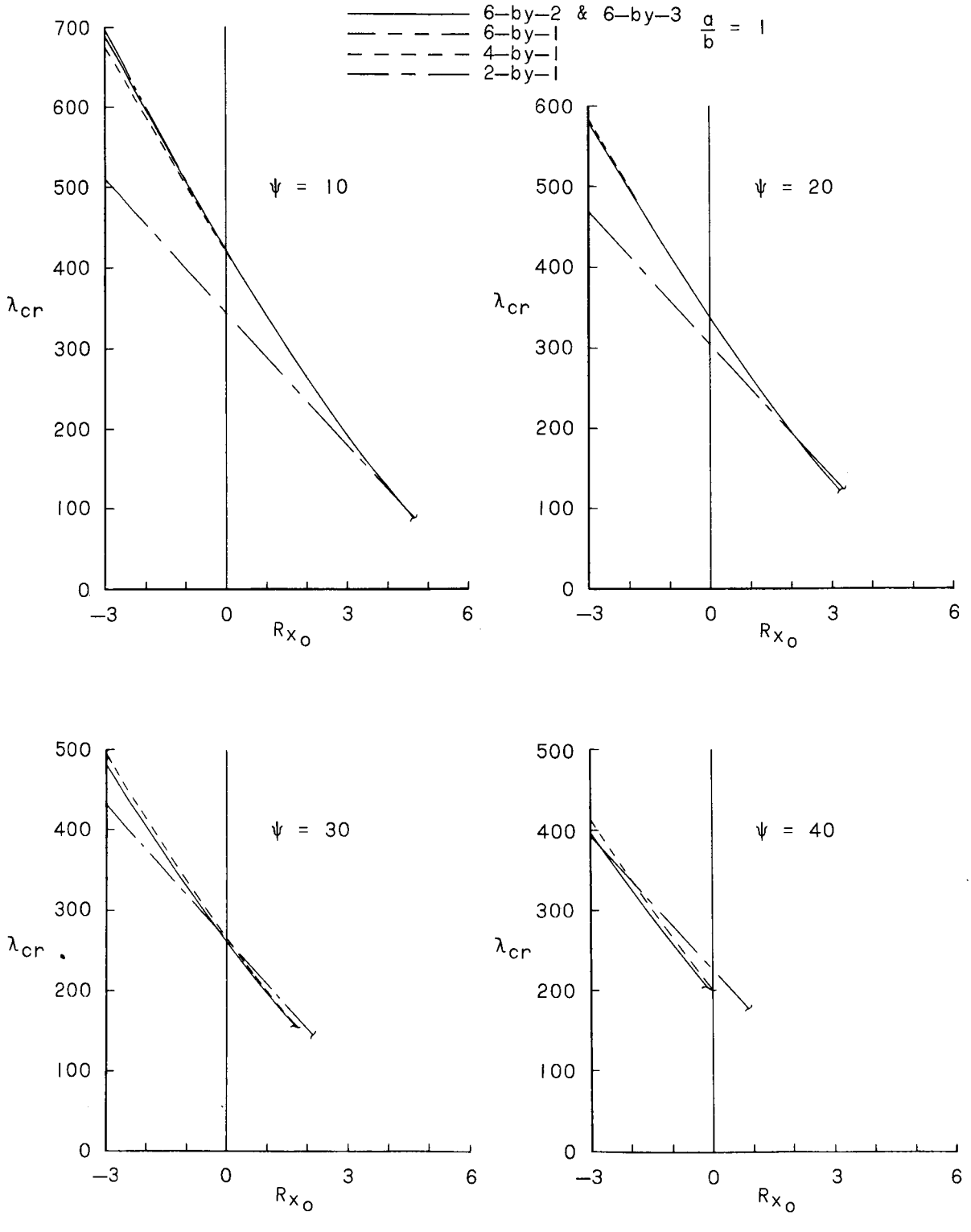

Figure 7.- Comparison of approximate solutions.

NASA-Langley, 1965 L-3845